NURETH14-078

APPLICATION OF ANT COLONY OPTIMIZATION APPROACH TO SEVERE ACCIDENT MANAGEMENT MEASURES OF MAANSHAN NUCLEAR POWER PLANT

C.-M. Tsai and S.-J. Wang

Institute of Nuclear Energy Research, Taiwan, R.O.C.

Abstract

The first three guidelines in the Maanshan SAMG were respectively evaluated for the effects in the SBO incident. The MAAP5 code was used to simulate the sequence of events and physical phenomena in the plant. The results show that the priority optimization should be carried out at two separated scenarios, i.e. the power recovered prior or after hot-leg creep rupture. The performance indices in the ant colony optimization could be the vessel life and the hydrogen generation from core for ant colony optimization.

Introduction

The Maanshan is a typical Westinghouse pressurized water reactor (PWR) nuclear power plant (NPP) with a large and dry containment. In order to improve the response capability for severe accidents, the Institute of Nuclear Energy Research cooperated with Taiwan Power Company to develop the severe accident management guidances (SAMGs) for the existing NPPs in Taiwan. The development of Maanshan SAMG [1] is based on the generic materials of the Westinghouse Owners Group (WOG) SAMG [2] with MAAP4 code [3]. The transition point from the emergence operating procedure (EOP) to SAMG phase is set as the core exit temperature over 922 K. In Taiwan the MAAP4 code was used to investigate the strategy of containment flooding of the Kuosheng NPP [4] and to validate the severe accident guidelines of the Chinshan NPP [5, 6].

The Maanshan SAMG consists of three parts, i.e. control room SAMG, Technical Support Center (TSC) severe challenge response guidance, and TSC SAMG in order. A Diagnostic Flow Chart (DFC) and a Severe Challenge Status Tree (SCST) are designed as references for the TSC staff to determine an appropriate strategy at the accident status. The DFC is a tool for diagnosis of plant condition or status in relation to a controlled stable condition and for the early diagnosis of potential challenges to containment fission product boundaries. The SCST is a tool for diagnosis of ongoing fission product releases and challenges to fission product boundaries. Four severe challenge guidelines (SCGs) in SCST are evolutionary and separate as same as the eight severe accident guidelines (SAGs) in the DFC. So far, there is no effective methodology available to verify and validate the priority of SAGs to accomplish the best mitigation.

The Ant Colony Optimization (ACO) algorithm is a meta-heuristic method and successfully applied to solve the combinatorial optimization problems, e.g. loading pattern problem [7]. The MAAP code is updated to fifth official version in 2010. The combination of the ACO

algorithm and the MAAP5 code to determine the optimal sequence of Maanshan SAGs is straightforward. Before that, the potential effects of respective SAGs in the SBO incident are evaluated in this study.

1. Maanshan SAMG

The Maanshan NPP employs two Westinghouse three-loop PWRs rated at 2,775 MWt. Three power-operated relief valves (PORVs) are associated with the pressurizer. The emergency core cooling system (ECCS) includes three accumulators (one for each reactor coolant loop), three centrifugal charging pumps (CCPs) for high-pressure injection and recirculation, and two residual heat removal (RHR) pumps for low-pressure injection and recirculation. Two of CCPs are used in normal operation and the rest one CCP is used for standby. The auxiliary feed water system, which consists of two motor-driven auxiliary feed water pumps (MDAFPs) and one turbine-driven auxiliary feed water pump (TDAFP), is used to supply water to the S/G secondary side when the main feed water pumps (MFPs) are unavailable. The Maanshan NPP employs a dry, prestressed concrete, steel-lined structure containment. The containment is equipped with a containment spray system and a containment fan cooler system to control the containment pressure and temperature during an accident. There are 39 thermocouples to measure the core exit temperature.

The SAMG development of the Maanshan NPP is based on the WOG SAMG generic materials. There are eight SAGs in the Maanshan SAMG. Figure 1 shows the DFC in which the consecutive check points and the corresponding SAG are summarized in Table 1. The first check point is the S/G water level below 71.2% capability. The corresponding SAG-1 is recommended to inject water to the S/G secondary side to prevent the S/G tube from rupture, scrub the fission products if tube rupture, and provide heat sink for the primary side. The second check point is RCS pressure over 28.12 kg/cm². The corresponding SAG-2 is recommended to depressurize the RCS to prevent high-pressure melt ejection, prevent S/G tube rupture, permit low-pressure injection, and increase the high-pressure injection rate. The following check point is core exit temperature over 371 °C (644 K). The corresponding SAG-3 is recommended to inject water into RCS to remove the stored energy and decay heat, prevent/delay reactor pressure vessel damage, and scrub the fission products. These three SAGs are focused on retaining the vessel integrity.

If the implementation of SAGs-1 through -3 was unavailable to mitigate the consequence, the following SAGs-4 to -8 are recommended to retain the containment integrity. In order to ensure that the emergency response staff is aware of the containment water inventory which is recommended to enhance the potential for reaching a controlled stable state with the core inside the reactor vessel, the SAG-4 "CONTAINMENT INJECTION" should be carried out if the containment water level is less than 5%. At the followed step, the emergency staff being aware of any significant releases from the plant can be ensured by the implementation of SAG-5 "REDUCING FISSION PRODUCT RELEASES" if the offsite whole body dose over 1 mSv and thyroid dose over 5 mSv. In order to ensure that the emergency response staff is aware of the containment pressure required for reaching a controlled stable state, the SAG-6 "CONTAINMENT TEMPERATURE & PRESSURE CONTROL" should be carried out if containment pressure over 0.22 kg/cm². At the followed step, the emergency staff being aware of the hydrogen concentration in the containment which is recommended for reaching a

controlled stable state can be ensured by the implementation of SAG-7 "HYDROGEN CONTROL" if the containment hydrogen concentration over 4%. In order to ensure the containment water inventory reaches the potential for a controlled stable state if the RPV should fail, the SAG-8 "CONTAINMENT FLOODING" is recommended to retain the containment water inventory over 11.31 m of height.

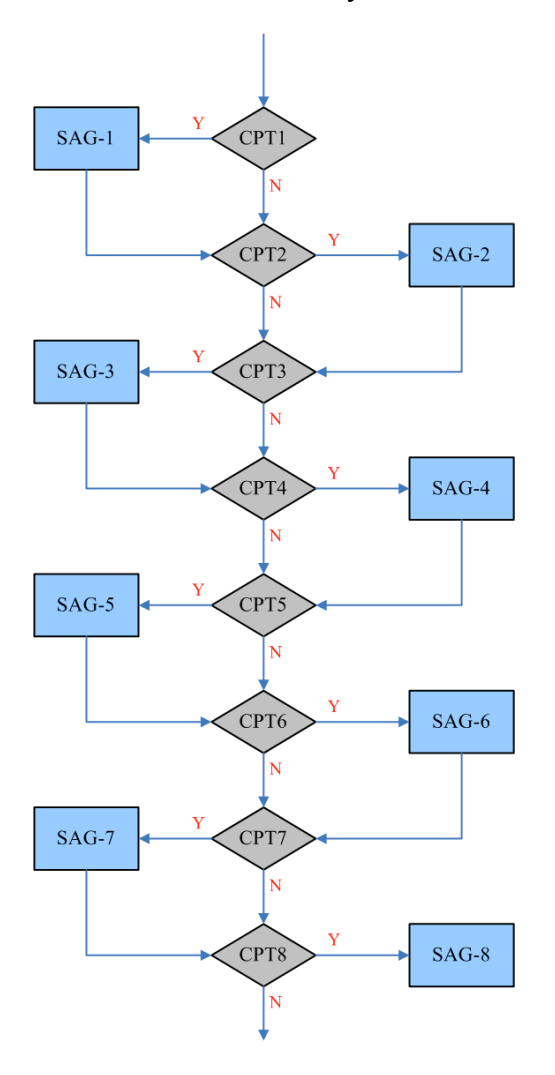


Table 1 Remarks for the diagnostic flow chart in the Maanshan SAMG.

Check Point	
CPT1	S/G water level < 71.2%WR
CPT2	RCS pressure > 28.12 kg/cm ²
CPT3	$CET > 371^{\circ}C (644 K)$
CPT4	Containment water level < 5%
СРТ5	Explant dose $D_w > 1 \text{ mSv}$
	$D_{thy} > 5 \text{ mSv}$
CPT6	Containment pressure $> 0.22 \text{ kg/cm}^2$
CPT7	Hydrogen concentration > 4%
CPT8	Containment water level < 10.31 m
	& no effective strategies
Severe Accident Guideline	
SAG-1	S/G injection
SAG-2	RCS depressurization
SAG-3	RCS injection
SAG-4	Containment injection
SAG-5	Reducing fission product release
SAG-6	Containment temperature &
	pressure control
SAG-7	Hydrogen control
SAG-8	Containment flooding

Figure 1 Diagnostic flow chart in the Maanshan SAMG.

2. Ant colony optimization

The ant colony optimization (ACO) algorithm, which is an optimization technique introduced in early 1990s. The RAS is a variant of the ACO algorithm, which contains two algorithmic components, ant based solution construction and pheromone update, in each iteration [8]. In the ant based solution construction, artificial ants can assemble solutions as sequences of solution components by probabilistic constructive heuristics. At each construction step, the choice of a solution component from a set of probable components is performed

probabilistically with respect to the pheromone model that called the transition probabilities. The transition probabilities are defined as follows [9].

$$p(c_i \mid s) = \frac{\left[\tau_i\right]^k \left[\eta(c_i)\right]^\beta}{\sum_i \left[\tau_i\right]^k \left[\eta(c_i)\right]^\beta}$$
(1)

Where $p(c_i | s)$ is a probability of choosing c_i from a probable components set as the solution component at each solution construction step, s is a solution, τ_i is the pheromone concentration of c_i , and η is an optional weight function, the values of η are called heuristic information, are α , β the weights of the pheromone concentration (τ) and heuristic information (η) .

The RAS pheromone update rule contains two parts, pheromone evaporation and pheromone increase. Pheromone evaporation uniformly decreases all the pheromone concentrations as iteration is performed. On the other hand, the pheromone concentration of the chosen solutions will increase. The convergent solution is the one which possesses the highest pheromone concentration. To avoid local optima, the value of pheromone evaporation should be small so that there is more chance to search for the different search space. Pheromone increase allows one or more solutions from the current iteration, and/or from earlier iterations, which are used to increase the solution components' pheromone concentration. The pheromone update can be formed as follows [9].

$$\tau_i \leftarrow (1 - \rho)\tau_i + \rho \sum_{s \in S_{upd}} w_s F(s) \tag{2}$$

Where τ_i is the pheromone concentration of solution component c_i , $0 < \rho \le 1$ is the evaporation rate, F(s) is a quality function of solution s, w_s is the weighting factor of this quality function, and S_{upd} is a solution set that can be used to update the solution components' pheromone. The set S_{upd} consists of best m-1 (where $m-1 \le n_a$ and n_a is the number of the artificial ants for each iteration) solutions from the solutions of current iteration and the best-so-far solution s_{bs} . In Eq. (2), the weighting factor w_s is set as follows: for the best m-1 solution of the current iteration, $w_s=m-r$, where r is the quality function value rank (the one with largest quality function value has rank 1 and so one) of the solution s at the current iteration; for the weight of the best-so-far solution s_{bs} , $w_s = m$. According to this setting, the best-so-far solution has the highest influence on the pheromone update, and the influences of the best m-1 solutions of the current iteration are dependent on their ranks. In addition, the value of m is determined by the designer.

3. Results and Discussion

In this study we focused on the potential effects on the RPV integrity from the implementation of SAGs-1 to -3. A simplified SBO incident of the Maanshan NPP is chosen as a base case. The sequence of incident events is discussed in Section 3.1. The potential effects from the respective implementation of SAGs-1 to -3 are summarized in Section 3.2.

The optimization design of ACO based on the results in Section 3.2 is illustrated in Section 3.3. All simulations are carried out through the MAAP5 code.

3.1 The SBO base case with no SAGs

In the simplified SBO incident of the Maanshan NPP, the loss of AC and DC power is assumed to occur at the beginning of simulation. Table 2 shows the sequence of events in the first 40,000 s. After loss of AC and DC power, the reactor scram follows with the main feedwater pumps and reactor coolant pumps tripped. Main feedwater is stopped and the turbine stop valves are closed. The water inventory in the RCS is continuously boiled up to steam due to the decay power and the RCS pressure is increased. At 4,477 s the safety valves start to automatically open while RCS pressure over 17.235 MPa for adjusting pressure. The water level in the vessel is decreased and lower than the top of active fuel (TAF) at 7,153 s. The core temperature then increases to 644 K at 7,875 s. The hydrogen generation starts at 8,485 s due to the interaction between the steam and the fuel cladding. The fission products are leaked through gap release. While the core exit temperature is higher than 922 K, the incident evolutes to the SAMG phase. After 1,000 s the reactor core is completely uncovered and followed by the hot-leg creep rupture. At 25,862 s the vessel is failed due to creep rupture.

Phase Timing (sec) Accident event SBO accident occurs 0 4,281 S/G loop2 dryout Pressurizer safety valves act for adjusting 4,477 RPV pressure Q/T rupture disk failed 5,360 EOP phase $7,\overline{153}$ Core uncovered Max. core temp. > 644 K 7,875 H₂ generation 8,485 Gap release 9.122 Core exit temperature > 992 K 10,198 Core water level < 3.22 m (BAF)11.241 Unbroken hot leg creep rupture 11,850 SAMG phase 11,874 Accumulator injection Core plate failed 18,756 RPV failed 25,862

Table 2 Sequence of events in Maanshan SBO

The SBO incident was initiated at 0 s. The reactor power decreased rapidly to radionuclide decay power as the reactor scrammed. The in-vessel pressure and core exit temperature increased as the water in the RCS is heated by the decay power. As shown in Figure 2, the safety valves are automatically acted to adjust the in-vessel pressure. Figure 3 shows the response of the RCS water inventory. Since the steam release for pressure adjustments, the RPV water inventory decreased monotonically to TAF at 7,153 s. The water level eventually

reached the bottom of active fuel (BAF) at 11,241 s. The accumulator water was injected into the vessel while hot-leg creep rupture. As shown in Figure 4 the Maanshan status evolutes to the SAMG phase at 10,198 s as the core exit temperature over 922 K.

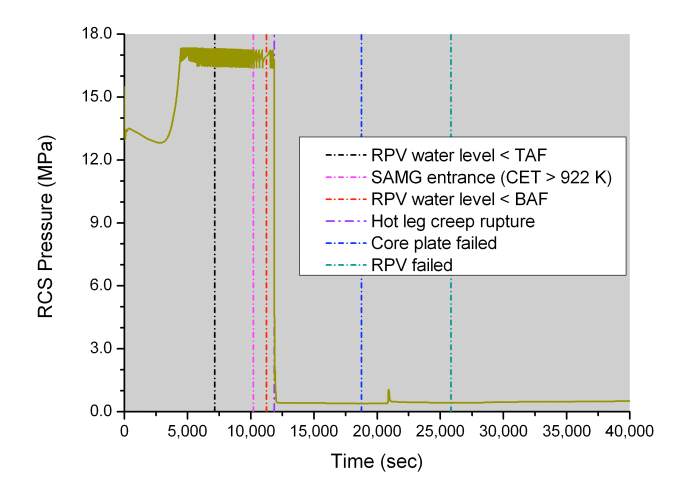


Figure 2 The response of the RCS pressure.

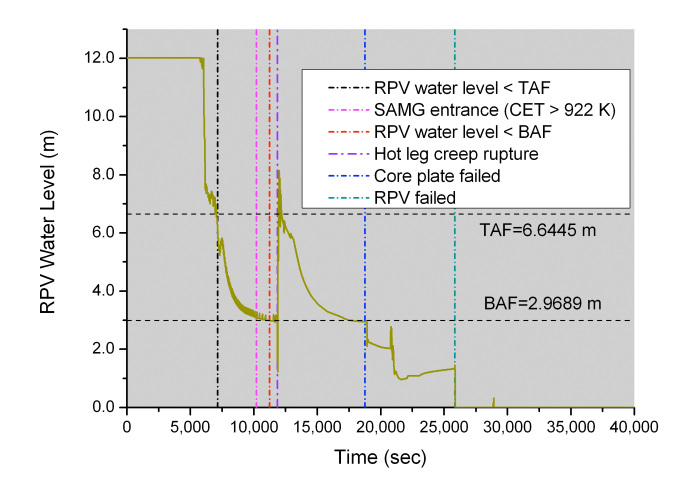


Figure 3 The response of the RPV water level.

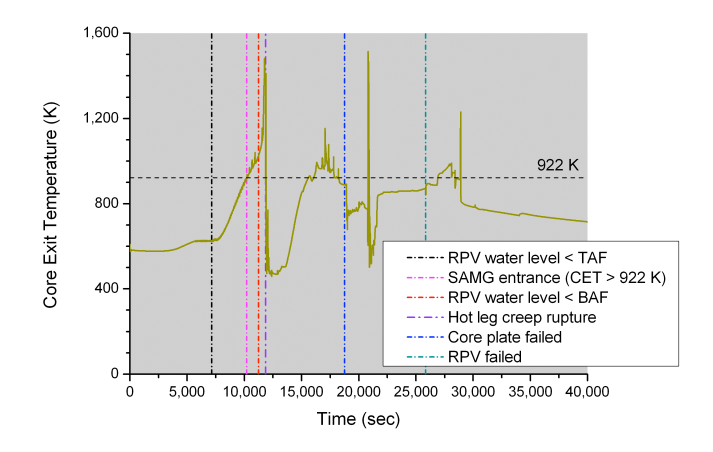


Figure 4 The response of the core exit temperature.

As the RPV water level fell below the TAF, the cladding temperature dramatically increased as the heat sink of the fuel decreased. The cladding temperature of the uncovered fuel rod increased earlier than that of the covered region. As the temperature over 1,100 K, the reaction of cladding oxidation began and the hydrogen was generated. Figure 5 shows the hydrogen generation in the SBO incident. Total 431.54 kg of hydrogen is generated with 51.4% cladding materials reacted in the vessel.

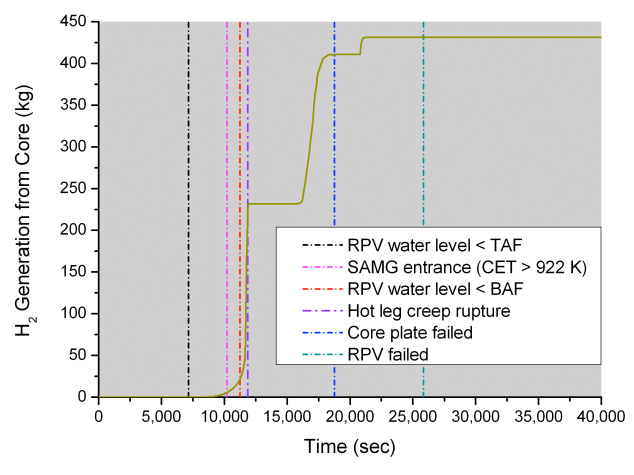


Figure 5 Hydrogen generation from core.

3.2 The SAG effects

This study is focused on the potential effects of SAGs-1 to -3 on the RPV integrity. In order to identify the design parameters, design merits, and optimization criteria, the respective SAG implementations for the SBO base case are studied. The AC and DC power are assumed to recover at 60 s after SAMG transition. The targeted performances are the RPV life and hydrogen generated from core.

S/G injection (SAG-1)

As the power recovery the motor-driven auxiliary feedwater pumps are turned on to inject the coolant into S/G secondary side to prevent tube rupture and provide a heat sink for the primary side. Through the water injection in the S/G secondary side, the RCS pressure decreased as the steam in the vessel is condensed to water. The water inventory in the accumulators is injected to the RCS to recover the core. The hydrogen generation is stopped while the fuel is fully covered. Only 8.83 kg of hydrogen is generated with 1.05% cladding materials reacted in the vessel.

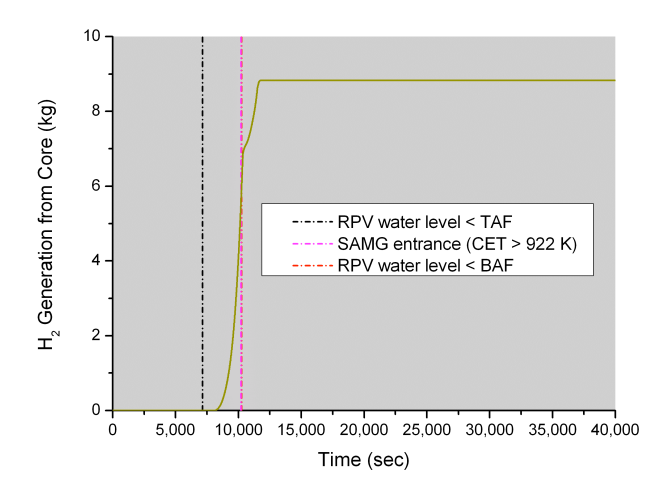


Figure 6 Hydrogen generation from core (SAG-1 introduced).

RCS depressurization (SAG-2)

At 60 s after power recovery, the PORVs on the pressurizer are manually opened to depressurize the RCS pressure. The water in the accumulators is injected to the RCS to recover the core for a while. After the accumulator water depleted, the cladding temperature rises again. Total 291.59 kg of hydrogen is generated with 34.73% cladding materials reacted in the vessel.

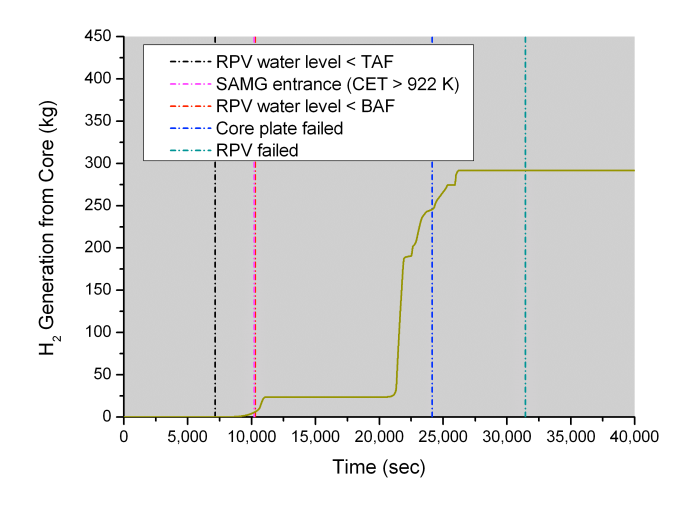


Figure 7 Hydrogen generation from core (SAG-2 introduced).

RCS injection (SAG-3)

At 60 s after power recovery, the charging pumps are turned on to provide high-pressure injection (HPI) to RCS. The hydrogen generation is stopped since the fuel recovered. The hotleg creep rupture, core plate failed, and RPV failure are eliminated.

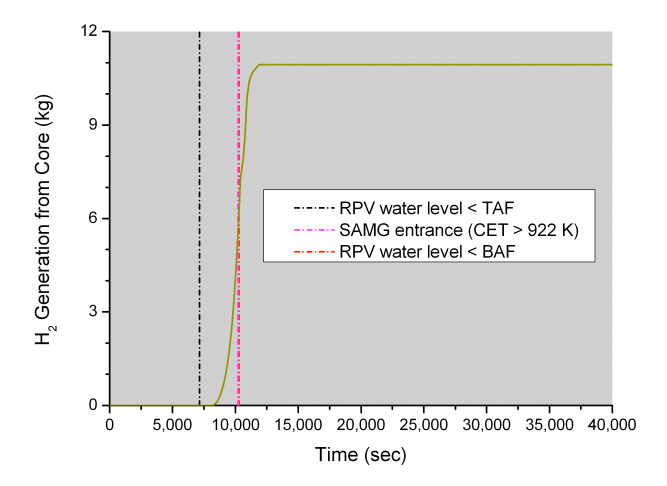


Figure 8 Hydrogen generation from core (SAG-3 introduced).

4. Conclusion

Through the implementation of any of SAGs-1 to -3, the hydrogen generation could be significantly reduced. The release reduction of fission products is also believed. The hot-leg creep rupture, core plate failed, and RPV failure are eliminated in the case of SAGs-1 and -3, while the capability of core support plate and the RPV integrity are extended. The performance indices should include eliminations of hot-leg creep rupture and RPV failure, the generation of hydrogen and fission products, and the vessel life if the RPV should fail.

As shown in Figure 2 the RCS pressure dramatically reduces to containment pressure due to hot-leg creep rupture. The hydrogen and fission products in the vessel can flow with the steam to the containment. The sequence of events for SAG implementation after hot-leg creep rupture may completely differ from the implementation prior to the creep rupture. Therefore, the priority optimization using the ACO algorithm should be carried out at two separated scenarios.

It's believed that the priority optimization of the Maanshan SAMG would be successfully determined by using the ACO algorithm with the results from this study.

5. References

[1] Taiwan Power Company, Severe Accident Management Guideline of Maanshan Nuclear Power Plant, Nov. 2002.

- [2] Westinghouse Electric Corporation, Westinghouse Owners Group Severe Accident Management Guidance, June 1994).
- [3] Fauske & Associates Inc., MAAP4-Modular Accident Analysis Program for LWR Power Plants, Jan. 2003.
- [4] W.-N. Su, S.-J. Wang, and S.-C. Chiang, "Investigation of Containment Flooding Strategy for Mark-III Nuclear Power Plant with MAAP4," Nuclear Technology, Vol. 150, pp. 251-262, 2005.
- [5] S.-J. Wang, T.-C. Wang, and S.-Y. Fann, Chinshan Severe Accident Management Guidelines, Rev. 2, Taiwan Power Company, 2003.
- [6] T.-C. Wang, S.-J. Wang, and J.-T. Teng, "Analysis of Severe Accident Management Strategy for a BWR-4 Nuclear Power Plant," Nuclear Technology, Vol. 152, pp. 253-265, 2005.
- [7] C.-D. Wang and C. Lin, "Automatic Boiling Water Reactor Loading Pattern Design Using ant Colony Optimization Algorithm," Annals of Nuclear Energy, Vol. 36, pp. 1151-1158, 2009.
- [8] B. Bullnheimer, R. F. Hartl, and C. Strauss, "A New Rank-based Version of the Ant System: A Computational Study," Central Eur. J. Oper. Res. Economy, Vol. 7, pp. 25-38, 1999.
- [9] C. Blum, "Ant Colony Optimization: Introduction and Recent Trends," Phys. Life, Vol. 2, pp. 353-373, 2005.